https://doi.org/10.5194/egusphere-2024-859
Preprint. Discussion started: 3 April 2024

Including the invisible: Deep depth-integrated chlorophyll estimates from remote sensing may assist in identifying biologically important areas in oligotrophic coastal margins

Renée P. Schoeman[1], Christine Erbe[1], and Robert D. McCauley[1]

[1]Centre for Marine Science and Technology, Curtin University, Bentley, Western Australia 6102, Australia

Correspondence to: Renée P. Schoeman (renee.koper@postgrad.curtin.edu.au)

Abstract. Deep chlorophyll maxima (DCM) are common in stratified water columns and may support higher trophic levels. Yet, it is challenging to include DCM contributions in studies aiming to identify marine animal foraging habitats and hotspots, because these studies often rely on satellite remote sensing data restricted to the surface. Previously established quantitative relationships between surface and depth-integrated chlorophyll within the euphotic zone of the open ocean and a eutrophic coastal margin encouraged us to assess whether such relationships are also present within the Western Australian intermittent-oligotrophic coastal margin. We also assessed whether the relationships could be extended to greater depths to capture DCMs below the euphotic zone. Based on ~9600 ocean glider profiles, our analyses demonstrate that such a relationship similarly exists off Western Australia and can be extended to twice the euphotic zone depth. Regression parameters were fine-tuned for three different conditions: 1) stratified waters in summer-transition months (September–April), characterised by relatively deep biomass maxima; 2) stratified waters in mid-winter (May–August) in which DCMs were less common and more likely a photo-acclimation maximum; and 3) mixed waters. While mean absolute errors increased in relationships over twice the euphotic zone depth (i.e., for estimates of deep depth-integrated chlorophyll), they remained low (i.e., max 16.5 %). These results and an observed chlorophyll increase in summer, unique to deep depth-integrated values, highlight the necessity to include deep depth-integrated chlorophyll estimates from satellite remote sensing in studies that aim to identify biologically important areas and productivity anomalies in (intermittent) oligotrophic environments.

1 Introduction

Phytoplankton are instrumental in providing energy to higher trophic levels of aquatic ecosystems. Their biomass is mostly quantified in terms of chlorophyll-*a* (hereafter called chlorophyll), from which primary productivity is derived, and areas with potentially high prey availability for higher trophic levels are identified (Huot et al., 2007; Hobday and Hartog, 2014). Indeed, several studies identified chlorophyll as a significant predictor variable of foraging habitat and hot spots for primary consumers (e.g., Schmidt et al., 2012; Hellessey et al., 2020) and higher trophic levels (e.g., Suryan et al., 2012; Palacios et al., 2019; Salgado Kent et al., 2020; Speakman et al., 2020).

https://doi.org/10.5194/egusphere-2024-859
Preprint. Discussion started: 3 April 2024

While chlorophyll levels can be quantified using several techniques (i.e., visual assessment of ocean colour, spectrophotometry, fluorometry, and chromatography; Parsons and Strickland, 1963; Yentsch and Menzel, 1963; Jeffrey, 1974; Gieskes and Kraay, 1977; Jeffrey et al., 1999), phytoplankton biomass and productivity studies flourished with the launch of the first satellite remote sensing ocean colour mission in 1978 (Hovis et al., 1980; McClain, 2009). Not only has satellite remote sensing generated a near-continuous chlorophyll dataset with high spatial resolution (Groom et al., 2019), but the data are also widely accessible, resulting in the inclusion of satellite-derived chlorophyll—almost as a default—in studies aiming to identify crucial marine animal foraging areas. Yet, satellite remote sensing is restricted to the upper water column and likely to exclude Deep Chlorophyll Maxima (DCMs; Gordon and McCluney, 1975; Smith, 1981), which may—at least in some areas—be an essential feature to support higher-order foraging efforts (Rennie et al., 2009a; Scott et al., 2010).

DCMs predominantly form in equatorial to subtropical regions between 35° N and 35° S, with increased seasonality when moving away from the equator (Cornec et al., 2021). The seasonality generally follows the seasonal occurrence of stable stratified water conditions (Cornec et al., 2021), in which light and nutrient availability drive the formation of true phytoplankton biomass maxima (i.e., deep biomass maxima, DBM) and deep photo-acclimation maxima (DAM; Mignot et al., 2014; Cullen, 2015). The latter results from an increased chlorophyll-to-carbon ratio because of low-light adaption rather than an increase in transferrable carbon (Steele, 1962, 1964) and is inherent to extreme oligotrophic systems (Cullen, 2015). However, both DCM types may contribute to water column productivity adequately enough to be of relevance to higher trophic levels (e.g., Weston et al., 2005; Fernand et al., 2013; Mignot et al., 2014; Marañón et al., 2021).

The marine habitat of Western Australia is characterised by a cross-shelf gradient in surface chlorophyll values decreasing from winter maxima ~1 mg m^{-3} along the coast to ~0.4 mg m^{-3} in offshore waters (i.e., >300 m deep; Lourey et al., 2006; Fearns et al., 2007; Hanson et al., 2007; Koslow et al., 2008). However, surface chlorophyll values vary seasonally and, offshore, generally do not exceed 0.1 mg m^{-3} in summer (Hanson et al., 2005b; Lourey et al., 2006; Koslow et al., 2008). These intermittent oligotrophic conditions result from the poleward flowing Leeuwin Current, which suppresses the upwelling of cold nutrient-rich water most of the time (Rennie et al., 2006, 2009b). DCMs form in the vertically stratified water column in summer at a depth between 50 m and 120 m offshore, shoaling to the surface or seabed on the continental shelf (Hanson et al., 2005a; Twomey et al., 2007; Koslow et al., 2008; Rennie et al., 2009a; Chen et al., 2019). While DCMs tend to break down around the shelf edge in late autumn and winter (Chen et al., 2019), they persist offshore at shallower depths (15-70 m; Hanson et al., 2005a; Koslow et al., 2008). Previous studies have confirmed that the DCM is often a biomass maximum (Hanson et al., 2005b, 2007; Rennie et al., 2009a), responsible for 30–70 % of total water column productivity (Hanson et al., 2007). More importantly, the DCM may be a vital feature for *Euphausia recurva*, the most abundant krill species along the southwest coast, including the Perth Canyon (Sutton and Beckley, 2016). Acoustic backscatter data from the Perth Canyon suggests that krill gather at 300–500 m depth during the day, rising to the DCM at night to feast on phytoplankton prey (Rennie et al., 2009a). Sutton (2015) supported this observation with fatty acid and stable isotope analysis on krill caught in the Perth Canyon, which did not reflect a diet of surface phytoplankton. *E. recurva*, in turn, is a known prey for both lantern fish (*Myctophum asperum*) and locally endangered pygmy blue whales (*Balaenoptera musculus brevicauda*) foraging in the Perth Canyon (Rennie et al.,

https://doi.org/10.5194/egusphere-2024-859
Preprint. Discussion started: 3 April 2024

2009a; Cohen and Beckley, 2021). Its apparent significance highlights the need to consider the inclusion of DCMs in phytoplankton biomass analyses.

Several studies have shown that surface chlorophyll values measurable by satellite remote sensing can estimate depth-integrated chlorophyll over the euphotic zone (i.e., measured as the depth over which Photosynthetically Active Radiation (PAR) decreases to 1 % of its surface value and noted as Z1%PAR; Morel and Berthon, 1989; Uitz et al., 2006; Frolov et al., 2012). However, these studies did not include data collected near Western Australia but samples from deep oceanic regions or a local eutrophic continental margin. In addition, $Z_{1\%}^{PAR}$ may underestimate the biological compensation depth at which the rate of photosynthesis equals that of autotrophic respiration and, thus, the depth of the productive layer (Wu et al., 2021). Consequently, regression analyses restricted to $Z_{1\%}^{PAR}$ may exclude DCMs.

This study aimed to assess whether depth-integrated chlorophyll can be estimated from surface chlorophyll levels measured over the intermittent oligotrophic continental margin of Western Australia, focusing on the area between 27.5° S and 33.8° S where the Perth Canyon lies. For such an assessment to be of value to future inferences of phytoplankton productivity (e.g., hotspots or anomalous productivity events) from satellite-derived surface chlorophyll data, it is imperative to ensure that depth-integrated values capture DCMs and that satellite remote sensing accurately reflects in situ conditions. While previous studies have touched on these topics, they were either spatiotemporally restricted (e.g., Hanson et al., 2005a, b, 2007; Fearns et al., 2007; Twomey et al., 2007; Koslow et al., 2008; Chen et al., 2019) or based on discontinued satellite data (i.e., SeaWIFS, concluded in 2010; Koslow et al., 2008). Hence, this study assessed temporal patterns in water column stratification, DCM formation, and DCM characteristics (i.e., type, depth, width); analysed the relationship between surface and depth-integrated chlorophyll values; and validated satellite-derived against in situ chlorophyll measurements.

2 Methods

2.1 In situ chlorophyll data retrieval

We obtained two in situ chlorophyll data sets through the Australian Ocean Data Network (AODN) portal for an area extending from 27.5° S to 33.8° S and 109.7° E to 115.4° E. One set comprised chlorophyll fluorescence data obtained with ocean gliders by the Integrated Marine Observing System's Australian National Facility for Ocean Gliders (IMOS-ANFOG; IMOS, 2023). The second set comprised chlorophyll concentration data obtained via High-Performance Liquid Chromatography (HPLC) and collated in the chlorophyll-a database of Australian waters (Davies et al., 2017, 2018). We restricted both datasets to samples collected between 04 July 2002 and 21 June 2022. Bathymetry data were extracted from the Australian bathymetry and topography grid (Whiteway, 2009), and all samples from waters <100 m deep were discarded to ensure only data from case 1 waters were included (i.e., water in which optical properties are driven by phytoplankton presence; Morel and Prieur, 1977). All data were processed in MATLAB (Version 2022b; The MathWorks Inc., 2022), while statistical analyses were performed in R and RStudio Statistical Software (V4.2.0 and V2023.03.0, respectively; R Core Team, 2022).

https://doi.org/10.5194/egusphere-2024-859
Preprint. Discussion started: 3 April 2024

2.2 Ocean glider depth profile extraction

Information extracted from ocean glider data samples included UTC date and time, latitude (DD), longitude (DD), sampling depth (m), chlorophyll concentration (mg m^{-3}), temperature (°C), practical salinity (‰), pressure (dbar), and profile phase (i.e., descent, inflexion, or ascent). Where available, particle backscattering coefficient data (m^{-1}) were also extracted. We filtered ocean glider data based on IMOS quality control flags to retain data points of which each variable was flagged as good data, probably good data, value adjusted by the quality control centre, or interpolated value (i.e., flags 1, 2, 5, and 8, respectively; Woo and Gourcuff, 2011). We then interpolated data between each decent and subsequent ascent phase to extract one vertical profile to the deepest recorded depth. Only profiles with at least one observation within the first 10 m of the water column and at least four samples at different depths were retained (Uitz et al., 2006). Finally, we calculated the sun's angle relative to the horizon for each profile with the *suncalc* R-package (Thieurmel and Elmarhraoui, 2022). Only profiles obtained with the sun below the horizon were included in further analyses to avoid underestimating surface chlorophyll concentrations because of non-photochemical quenching (Roesler and Barnard, 2013).

2.3 Temporal patterns in water column conditions

The prevalence of DCMs and the relationship between surface and depth-integrated chlorophyll concentrations differ in mixed and stratified water columns (Morel and Berthon, 1989; Uitz et al., 2006; Cullen, 2015). Thus, we split profiles between mixed and stratified water conditions based on the euphotic zone depth (i.e., $Z_{eu} = Z_{1\%}^{PAR}$; see Table 1 for a list of symbols) and the mixed layer depth (Z_{mld}) as positive values below the surface. Following Uitz et al. (2006), we classified waters as mixed when $Z_{eu}<Z_{mld}$ and stratified when $Z_{eu}>Z_{mld}$. The euphotic zone depth for each profile was derived from the vertical chlorophyll distribution by progressive trapezoidal integration of chlorophyll over depth (Z; Morel and Berthon, 1989). For each sampling depth (Z_i), we converted depth-integrated chlorophyll concentrations to euphotic zone depth with formulae in Morel and Maritorena (2001) until $Z_{eu}<Z_i$ (Morel and Berthon, 1989). The exact euphotic zone depth was then calculated by interpolating Z_{eu} between Z_i and Z_{i-1} to find where Z equalled Z_{eu} (Morel and Berthon, 1989). Profiles that did not cover the euphotic zone were discarded.

Table 1: List of symbols used in this study and their denotation.

Symbol	Denotation	Unit
Bbp_{max}	Maximum backscattering coefficient within 20 m of the deep chlorophyll maximum.	m^{-1}
Bbp_{min}	Minimum backscattering coefficient within the top 15 m of the water column.	m^{-1}

https://doi.org/10.5194/egusphere-2024-859
Preprint. Discussion started: 3 April 2024

Chl_{HPLC}	Average chlorophyll concentration within the top 10 m of the water column obtained from High-Performance Liquid Chromatography analyses of in situ water samples.	mg m^{-3}
Chl_{max}	Maximum chlorophyll concentration within the top 300 m of the water column.	mg m^{-3}
Chl_{MODIS}	Surface chlorophyll concentration retrieved with the OCI algorithm from ocean colour measurements by MODIS-aqua.	mg m^{-3}
Chl_{zeu}	Total chlorophyll concentration integrated over the euphotic layer.	mg m^{-2}
Chl_{zeu2}	Total chlorophyll concentration integrated over twice the euphotic layer depth.	mg m^{-2}
Chl_{zpd}	Average chlorophyll concentration within the first optical depth.	mg m^{-3}
DCM_{width}	Width of the deep chlorophyll maximum; calculated as the difference in depth between the shallow- and deep half-peak depths.	m
Z	Depth below the water surface (positive).	m
$Z_{1\%}^{PAR}$	Depth at which the Photosynthetically Active Radiation (PAR) is 1 % of its surface value.	m
Z_{DCM}	Depth of Chl_{max}.	m
Z_{DCM50d}	Closest depth to Z_{DCM} at which chlorophyll concentration decreased to 50 % of Chl_{max}; deep half-peak width.	m
Z_{DCM50u}	Closest depth to Z_{DCM} at which chlorophyll concentration increased to 50 % of Chl_{max}; shallow half-peak width.	m
Z_{eu}	Bottom depth of the euphotic layer (in this study equal to $Z_{1\%}^{PAR}$).	m
Z_{mld}	Bottom depth of the water column mixed layer.	m

Raw temperature, salinity, and pressure data were converted to potential temperature and density values with the Gibbs-
120 SeaWater (GSW) Oceanographic Toolbox (IOC et al., 2010; McDougall and Barker, 2020) to calculate the mixed layer depth. Here, we define the mixed layer depth as the first depth at which either the potential temperature differed by 0.2 °C from the reference potential temperature or the potential density exceeded the reference potential density by 0.03 kg m^{-3} (de Boyer Montégut et al., 2004; Boettger et al., 2018). Samples taken at 10 m depth were used as reference values (Boettger et al., 2018).

https://doi.org/10.5194/egusphere-2024-859
Preprint. Discussion started: 3 April 2024

2.4 Temporal patterns in DCM presence, classification, and characteristics

Identification and classification of DCMs for individual profiles followed methods in Cornec et al. (2021), so we only briefly describe the methods here. We assumed a DCM was present if the maximum chlorophyll concentration (Chl_{max}) within the top 300 m exceeded twice the median chlorophyll concentration over the first 15 m (Cornec et al., 2021). For each DCM, we extracted the depth of Chl_{max} (Z_{dcm}; DCM peak depth), the shallow half-peak depth (Z_{dcm50u}), and the deep half-peak depth (Z_{dcm50d}). The half-peak width (DCM_{width}) was subsequently calculated as the depth range between the shallow and deep half-peak depths (i.e., $Chl_{max} \pm 0.5 \times Chl_{max}$; Li et al., 2022). Trends in the position of the DCM relative to the euphotic zone were assessed by calculating the relative DCM depth as Z_{dcm50d}/Z_{eu}; values <1 indicate that the full half-peak width fell within the euphotic zone. Where backscattering coefficient data were available, the maximum backscattering coefficient (Bbp_{max}) within 20 m of the DCM was compared to the minimum backscattering coefficient (Bbp_{min}) in the top 15 m (Cornec et al., 2021). When Bbp_{max} exceeded 1.3 times Bbp_{min}, we assumed the DCM was a DBM. Otherwise, the DCM was considered a DAM.

2.5 Relationships between surface and (deep) depth-integrated chlorophyll

Relationships between surface and depth-integrated chlorophyll concentrations were assessed based on methods described in earlier publications (Morel and Berthon, 1989; Uitz et al., 2006; Frolov et al., 2012). We calculated surface chlorophyll values—assumed measurable by satellite—as the average chlorophyll concentration over the first optical depth (i.e., Chl_{zpd}; Uitz et al., 2006), where the first optical depth refers to $Z_{eu}/4.6$ (Gordon and McCluney, 1975). Depth-integrated chlorophyll concentrations were calculated over the euphotic zone (Chl_{zeu}; hereafter referred to as "depth-integrated chlorophyll") and twice the euphotic zone depth (Chl_{zeu2}; hereafter referred to as "deep depth-integrated chlorophyll") with trapezoidal integration. The latter differs from Uitz et al. (2006), who only integrated chlorophyll over a maximum of one-and-a-half times the euphotic zone depth because preliminary analysis indicated that only 60 % of DCM half-peak widths fell within that limit. Relationships were quantified with linear regression analyses on log_{10} transformed data separately for mixed and stratified water conditions. Previous publications used two regression lines to quantify the relationship in stratified waters because of a change in slope at surface chlorophyll values ~1 mg m^{-3} (Morel and Berthon, 1989; Uitz et al., 2006; Frolov et al., 2012). While preliminary data analysis revealed a similar change in slope for stratified waters in this study, this change in slope appeared seasonal; thus, we carried out one regression analysis for stratified water conditions from September until April and one for stratified water conditions from May until August. For brevity, the two seasons will be referred to as summer-transition and mid-winter, respectively. We evaluated all models with the Mean Absolute Error (MAE) and bias metrics because of tailed distributions in model residual plots (Chai and Draxler, 2014; Seegers et al., 2018; Hodson, 2022). Both metrics were transformed from linear to multiplicative values for ease of interpretation (Seegers et al., 2018). The slope and intercept of the linear regression were used to describe the non-linear relationship between non-transformed surface and (deep) depth-integrated chlorophyll values with a power law regression.

https://doi.org/10.5194/egusphere-2024-859
Preprint. Discussion started: 3 April 2024

2.6 Satellite data match-up and validation

In situ measurements obtained with HPLC analysis were filtered to retain samples collected from the top 10 m of the water column (Sathyendranath et al., 2019). Replicated and depth profile samples were averaged to one measurement per station in time (i.e., Chl_{HPLC}). Further filtering included removing spurious values >1.8 mg m^{-3} that fell outside the typical range reported for this area (i.e., ≤1 mg m^{-3}; Lourey et al., 2006; Koslow et al., 2008; Thompson et al., 2011). Satellite-derived chlorophyll concentrations (i.e., Chl_{MODIS}) were extracted from data collected with the NASA Moderate Resolution Imaging Spectroradiometer onboard Aqua (i.e., MODIS-aqua[1]). Satellite values were derived using the OCI algorithm that applies the OC3M band-ratio algorithm for retrieval of Chl_{MODIS}>0.35 mg m^{-3}, the band difference Color Index (CI) for retrieval of Chl_{MODIS}<0.25 mg m^{-3}, and a weighted approach to retrieve 0.25≤Chl_{MODIS}≤0.35 mg m^{-3} (Hu et al., 2012, 2019; O'Reilly and Werdell, 2019).

Satellite data were validated against in situ data via a match-up process. The match-up process started by searching for level 2 (i.e., L2) satellite granules within the Earth Data Common Metadata Repository, based on in situ sampling locations and a 24 h threshold time difference. All candidate L2 files were extracted from the Ocean Biology Distributed Active Archive Center (OB.DAAC) with Ocean Color Science Software Processors (OCSSW) V2022.3 running in SeaDAS 8.3.0. The following step extracted a box of 3×3 pixels centred on the in situ sampling location and validated each pixel based on the viewing angle (i.e., ≤60°), solar zenith angle (i.e., ≤70°), and standard processing flags (i.e., no cloud cover, cloud shadow, sun glint, stray light, extreme top-of-atmosphere radiance, or atmospheric correction failure; Bailey and Werdell, 2006; Zibordi et al., 2009). Successful match-ups were identified as those with at least six valid pixels and a maximum spatial variability of 15 % around the mean (i.e., coefficient of variation ≤0.15; Bailey and Werdell, 2006).

We assessed the linear relationship between log_{10} transformed satellite and in situ chlorophyll values with a Reduced Major Axis (RMA) regression analysis with 9999 permutations from the *lmodel2* R-package (Legendre, 2018). Model errors were normally distributed but increased at the extremes, identifying the MAE and bias as suitable validation metrics (Chai and Draxler, 2014; Seegers et al., 2018; Hodson, 2022).

3 Results

3.1 Temporal patterns in water column conditions

We extracted 6438 and 3234 profiles from stratified and mixed water conditions, respectively. Stratified water conditions dominated over the warm late spring and summer months (October–March; >85 % of profiles), declining to <35 % over May–July when mixed water conditions prevailed (Fig. 1). Transition conditions were present in April, August, and September. The

[1] NASA Goddard Space Flight Center, Ocean Ecology Laboratory, Ocean Biology Processing Group. Moderate-resolution Imaging Spectroradiometer (MODIS) Aqua Color Data; 2022 Processing. NASA OB.DAAC, Greenbelt, MD, USA; doi: https://doi.org/10.5067/AQUA/MODIS/L2/OC/2022

https://doi.org/10.5194/egusphere-2024-859
Preprint. Discussion started: 3 April 2024

change in prevailing water condition was predominantly caused by a shallowing of the euphotic zone depth from a mean of 68.6 m (SD 12.4; range 22.7–103.5) in October–March to 53.0 m (SD 9.3; range 32.7–100.7) in May–August. In contrast, the mean mixed layer depth deepened from 36.3 m (SD 19.2; range 10.5–161.5) to 62.5 m (SD 36.8; range 10.5–202.5), respectively.

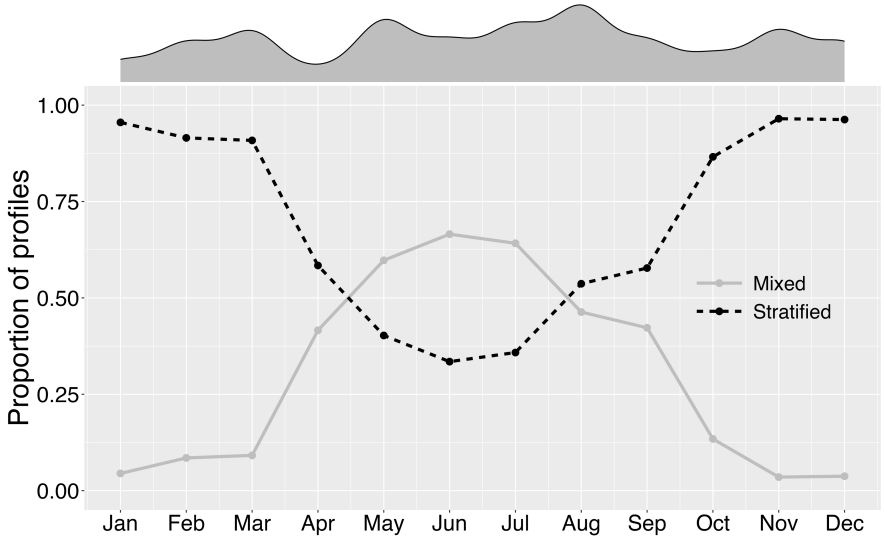

Figure 1: The proportion of chlorophyll profiles identified as coming from mixed (solid grey line) and stratified (dashed black line) water conditions for each month of the year. The density plot reflects the monthly profiles available, ranging from N = 214 to N = 1416 in April and August, respectively.

3.2 Temporal patterns in DCM presence, classification, and characteristics

Overall, DCMs formed between the surface and 178.4 m deep, at a mean depth of 76.5 m (SD 24.7). DCMs were common in stratified water conditions (~60 % of profiles; 3892/6438), where the formation followed a seasonal trend. From October until March, >75 % of profiles were characterised by a DCM, reducing to <20 % from May until August. April and September were transition months in which 33 % and 47 % of stratified profiles had a DCM, respectively. Backscattering data were available for 1985 stratified profiles with a DCM, revealing that DBMs were more common over September–March (58–75 % of DCMs) than over May–August (23–38 % of DCMs). There was a weak seasonal trend in mean DCM depth, with a deepening from 40.5 m (SD 23.2; range 7.0–80.0) in July to 83.0 m (SD 24.4; range 4.5–158.6) in December (Fig. 2). The DCM moved closer to the surface in January–March (68.4–75.1 m), before occupying a more variable depth from April to July (i.e., mean depth changed between 40.5 m and 80.2 m: Fig. 2). This seasonal trend in DCM depth was observed for both DCM types, but DAMs lay deeper than DBMs year-round. Consequently, the mean overall depth of DAMs (83.0 m; SD 21.9; range 18.3–169.1) exceeded that of DBMs (75.4 m; SD 24.1; range 3.3–73.4). Similarly, DAMs were generally more expansive than DBMs (especially in May–July), as reflected by the mean half-peak widths of 55.3 m (SD 24.0; range 12.8–152.2) and 44.8 m (SD

https://doi.org/10.5194/egusphere-2024-859
Preprint. Discussion started: 3 April 2024

24.9; range 0.5–143.1), respectively. Yet, regardless of DCM type, only 6 % of half-peak widths in stratified waters fell within the euphotic zone, increasing to 96 % when looking over twice the euphotic zone depth.

DCM formation in mixed water conditions was rare (~6 % of profiles; 195/3234), and profiles for which backscatter data were available revealed that these chlorophyll maxima were nearly always a DBM (91 %, 60/66). While DCMs in mixed water conditions were found at a variable depth (mean 83.0 m; SD 45.0; range 2.9–178.4), they were commonly thin (mean 19.4 m, SD 30.8, range 0.3–128.2). In fact, 66 % of all DCMs and 85 % of DBMs in mixed water conditions had a half-peak less than 5 m wide (i.e., $DCM_{width}<5$). DBMs were also more commonly found within the euphotic zone (55 %), while the limited observation of DAMs occurred mostly beyond the euphotic zone depth (80 %).

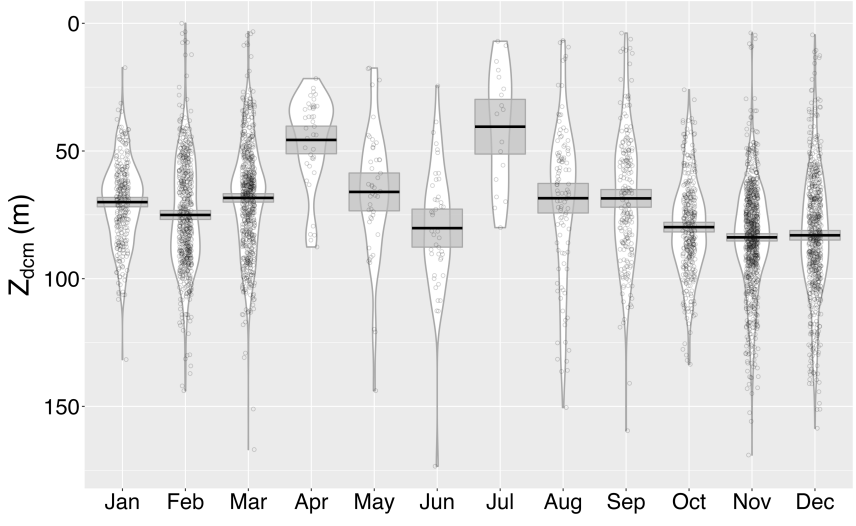

Figure 2: Mean depth of the Deep Chlorophyll Maximum (Z_{dcm}; black line) in stratified water columns per month of the year with 95 % confidence intervals (grey boxes). All data points are plotted as open grey circles, with white violins indicating the data density distribution.

3.3 Relationships between surface and (deep) depth-integrated chlorophyll

Surface chlorophyll concentrations ranged between 0.040 and 1.586 mg m^{-3} (mean 0.448 mg m^{-3}, SD 0.272). Monthly mean surface chlorophyll values peaked in May (mean 0.758 mg m^{-3}, SD 0.271), with relatively higher levels maintained in winter (i.e., monthly means >0.5 mg m^{-3}; Fig. 3a). A modest secondary increase occurs in August after which surface chlorophyll levels decrease to means <0.4 mg m^{-3} in summer. April and September can be considered as transition months. A similar seasonal pattern can be discerned for depth-integrated chlorophyll values, which ranged between 13.3 and 74.5 mg m^{-2} (Fig. 3b). Interestingly, while monthly mean deep depth-integrated chlorophyll similarly peaked in May (mean 61.5 mg m^{-2}, SD 13.6), the increase in August (mean 54.3 mg m^{-2}, SD 11.1) appears more pronounced and a third increase was present in January (mean 54.8 mg m^{-2}, SD 9.4; Fig. 3b).

https://doi.org/10.5194/egusphere-2024-859
Preprint. Discussion started: 3 April 2024

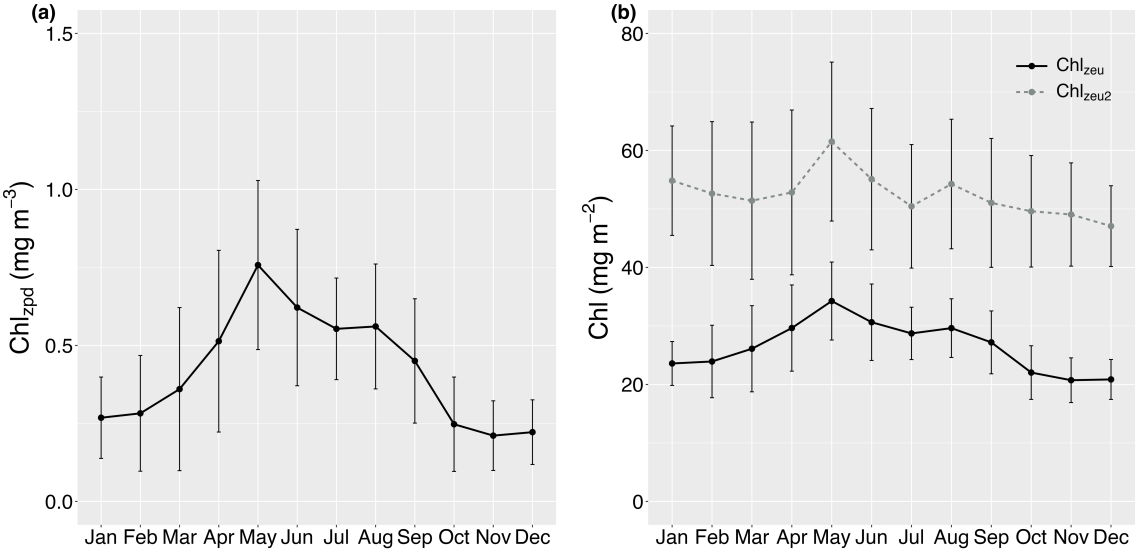

Figure 3: Monthly mean surface (Chl_{zpd}; panel a), depth-integrated (Chl_{zeu}; black solid line in panel b) and deep depth-integrated (Chl_{zeu2}; grey dashed line in panel b) chlorophyll values. Error bars represent the standard deviations to illustrate the data variation around the mean.

Profiles collected from stratified water conditions in summer-transition months showed a significant linear relationship between surface and depth-integrated chlorophyll concentrations ($R^2 = 0.73$, $F_{(1,4574)} = 12370$, $p<0.001$; Fig. 4a). A stronger relationship with a steeper slope and less scatter was seen for the cooler months (mid-winter; $R^2 = 0.88$, $F_{(1,1857)} = 13400$, $p<0.001$; Fig. 4b). Models estimated observed depth-integrated chlorophyll values with mean relative errors of 9.0 % and 6.0 %, respectively (i.e., MAE: 1.090 and 1.060, respectively). Scatter in the data increased for deep depth-integrated values, resulting in a weak linear relationship in summer-transition months ($R^2 = 0.22$, $F_{(1,3302)} = 920.5$, $p<0.001$; Fig. 4c) and a moderate relationship in mid-winter ($R^2 = 0.52$, $F_{(1,1674)} = 1808$, $p<0.001$; Fig. 4d). The mean relative errors increased to 16.3 % and 15.7 %, respectively. The derived non-linear relationships are summarised in Table 2.

https://doi.org/10.5194/egusphere-2024-859
Preprint. Discussion started: 3 April 2024

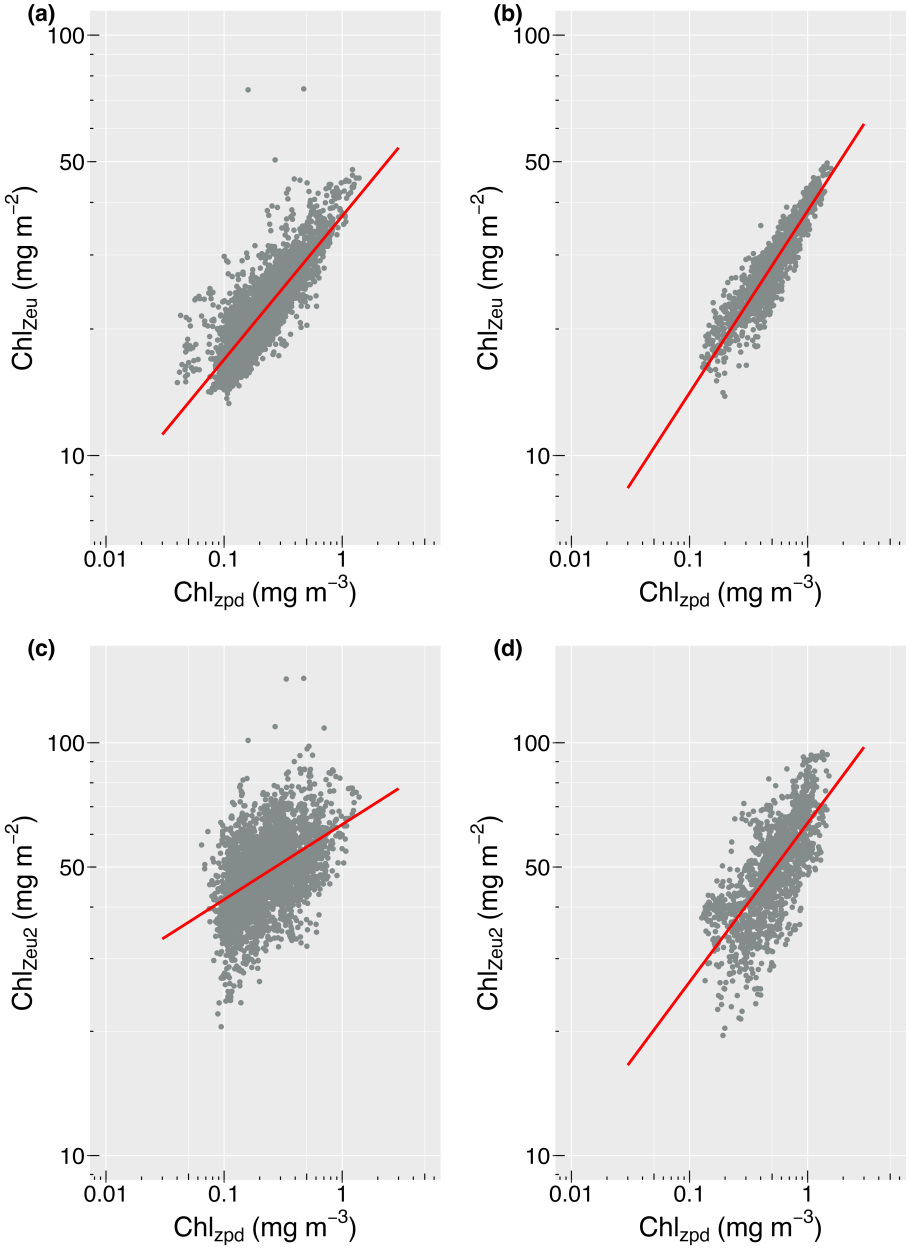

Figure 4: Relationship between surface (Chl_{zpd}) and depth-integrated (Chl_{zeu}) vs. deep depth-integrated (Chl_{zeu2}) chlorophyll values for summer-transition (i.e., September–April; a, c) and mid-winter months (i.e., May–August; b, d) in stratified waters. Red lines indicate the derived regression lines. Note the change in the y-axis range between panels a–b and c–d.

Profiles from mixed water conditions revealed a strong linear relationship between surface and depth-integrated values over the euphotic zone ($R^2 = 0.97$, $F_{(1,3230)} = 105700$, $p<0.001$; Fig. 5a). The slope was steeper than that observed in stratified water (i.e., 0.521 against 0.343 and 0.433; Table 2Table) and data were concentrated around the regression line, resulting in a low

https://doi.org/10.5194/egusphere-2024-859
Preprint. Discussion started: 3 April 2024

MAE of 1.018 (i.e., 1.8 % relative error) without bias. As for stratified water, scatter in the data increased for deep depth-integrated values, but a moderate relationship was still found ($R^2 = 0.65$, $F_{(1,2797)} = 5220$, $p<0.001$; Fig. 5b) with an increase in mean relative error to 8.6 %.

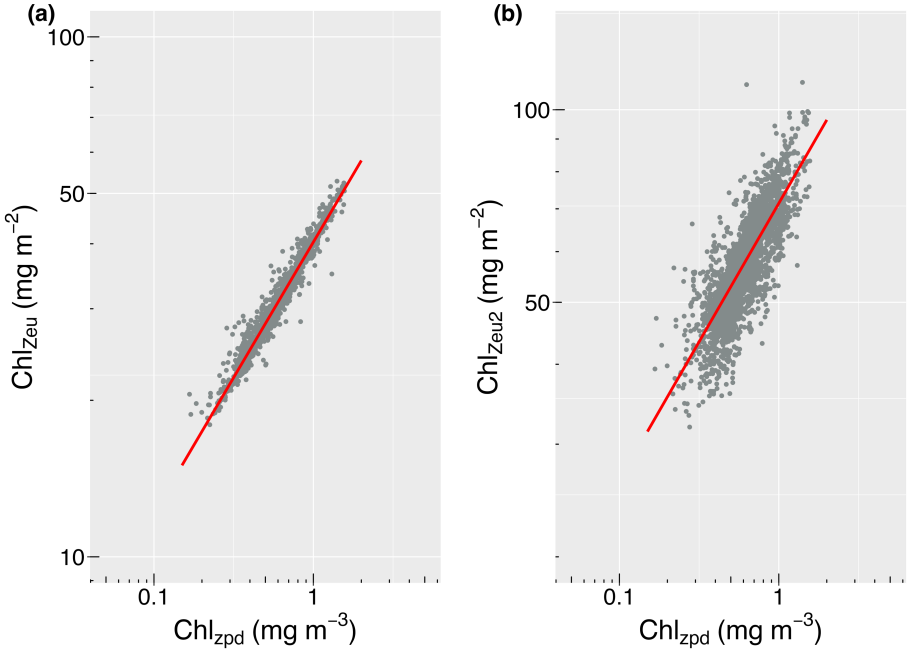

Figure 5: Relationship between surface (Chl_{zpd}) and depth-integrated (Chl_{zeu}; a) vs. deep depth-integrated (Chl_{zeu2}; b) chlorophyll values in mixed waters. Red lines indicate the derived regression lines. Note the change in the y-axis range between panels.

Table 2: Summary of non-linear relationships between surface (Chl_{zpd}) and depth-integrated (Chl_{zeu}) vs. deep depth-integrated (Chl_{zeu2}) chlorophyll under stratified and mixed water conditions. Relationships in stratified waters are given for both summer-transition (i.e., September–April) and mid-winter months (May–August).

Water condition	Integration depth	Regression	R^2	MAE	Bias
Stratified					
Summer-Transition	Z_{eu}	$Chl_{zeu} = 37.1 \times Chl_{zpd}^{0.341}$	0.73	1.090	1.00
Mid-Winter	Z_{eu}	$Chl_{zeu} = 38.2 \times Chl_{zpd}^{0.433}$	0.88	1.060	1.00
Summer-Transition	Z_{eu2}	$Chl_{zeu2} = 63.4 \times Chl_{zpd}^{0.182}$	0.22	1.163	1.00
Mid-Winter	Z_{eu2}	$Chl_{zeu2} = 63.9 \times Chl_{zpd}^{0.385}$	0.52	1.157	1.00
Mixed					
Year-round	Z_{eu}	$Chl_{zeu} = 40.3 \times Chl_{zpd}^{0.521}$	0.97	1.018	1.00
Year-round	Z_{eu2}	$Chl_{zeu2} = 71.4 \times Chl_{zpd}^{0.433}$	0.65	1.086	1.00

https://doi.org/10.5194/egusphere-2024-859
Preprint. Discussion started: 3 April 2024

3.4 Satellite data match-up and validation

We identified 61 valid match-ups under the 24 h time-difference threshold, with in situ chlorophyll measurements ranging between 0.07 and 0.67 mg m^{-3}. The RMA regression confirmed a positive relationship between satellite and in situ data with scatter around the regression line (R^2 = 0.66; Fig. 6). The OCI algorithm predicted satellite values on average within 32 % accuracy of observed measurements (MAE = 1.32). While an overestimation in satellite values can be discerned at Chl_{HPLC}<0.17 mg m^{-3}, the OCI algorithm underestimated measured chlorophyll on average by 1 % (bias = 0.99).

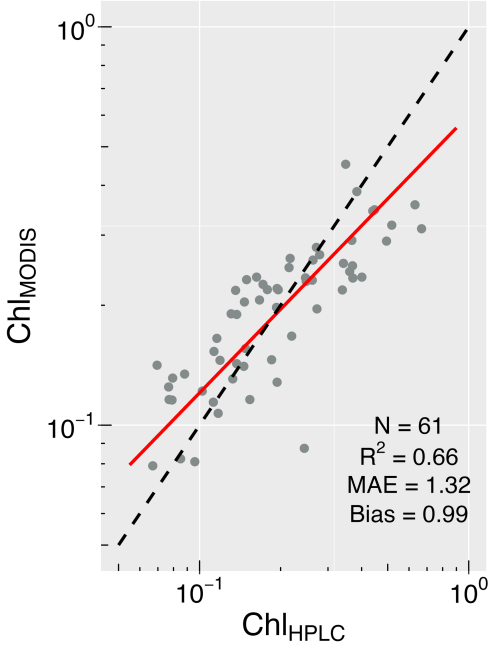

Figure 6: Chlorophyll data derived from MODIS-aqua with the OCI algorithm (Chl_{MODIS}) plotted against in situ chlorophyll measurements obtained with HPLC analyses (Chl_{HPLC}). Reduced Major Axis (RMA; red line) and 1:1 ratio (black dashed line) visualise the error trend.

4 Discussion

Several studies have highlighted that in oceanic regions (Morel and Berthon, 1989; Uitz et al., 2006) and over eutrophic continental margins (Frolov et al., 2012), the relationship between surface and depth-integrated chlorophyll in stratified and mixed waters can be approximated with a power law regression. Here, we used in situ ocean glider data to demonstrate that such a relationship similarly exists over the intermittent oligotrophic continental margin of Western Australia and can be extended to twice the euphotic zone depth, albeit with higher uncertainty when integrating over greater depths. Regression parameters were extracted for 1) stratified waters in summer-transition months (September–April), characterised by relatively

https://doi.org/10.5194/egusphere-2024-859
Preprint. Discussion started: 3 April 2024

deep DBMs, 2) stratified waters in mid-winter (May–August) in which DCMs were less common and more likely a DAM, and 3) mixed waters.

Ocean glider data revealed that stratified water with a DCM dominated in summer, while a more balanced occurrence of mixed and stratified waters with a reduced probability of DCMs was observed during transition months and in mid-winter. DCM depth similarly varied seasonally from relatively stable deep DCMs in summer to more variable depths in mid-winter. These seasonal changes are typical at the 30–50° latitudinal bands (Cornec et al., 2021) because winter surface cooling and wind-induced mixing deepen the mixed layer (Kara et al., 2003; de Boyer Montégut et al., 2004), while an increase in surface chlorophyll and reduced solar irradiance cause a shallowing of isolumes (i.e., level where the daily integrated photon flux is constant) and the associated DCM (Mignot et al., 2014). In the area surrounding the Perth Canyon, north-westerly down-welling favourable storms (wind speeds >15 m s^{-1}; most frequent June–August) mix the water column down to 200 m depth, breaking down the stratified layer and DCM (Rennie et al., 2006; Chen et al., 2020). Re-stratification occurs during subsequent calm post-storm south-westerly winds (wind speeds <7 m s^{-1}; Rennie et al., 2006), allowing for the reformation and progressive deepening of DCMs as the stratification intensifies. Warm-core eddies are also known to generate well-mixed layers extending beyond the euphotic zone depth (Pearce and Griffiths, 1991; Thompson et al., 2007). Both short- and long-lived warm-core eddies are formed year-round along the Western Australian coast (Pearce and Griffiths, 1991; Fang and Morrow, 2003), but are more frequent between 28° and 31° S in late autumn and winter (Fang and Morrow, 2003). Thus, wind-induced mixing and more frequent eddy formation likely contributed to the more pronounced occurrence of mixed water conditions without DCMs in mid-winter.

While DCM formation is always at least in part caused by photo-acclimation of phytoplankton to low light conditions (Cullen, 2015), deep DCMs in summer may approach the nitracline, allowing for phytoplankton growth and thus, DBM formation (Mignot et al., 2014). Summer DBMs in the Leeuwin Current and offshore waters of Western Australia have indeed been found to approach the nitracline (Hanson et al., 2005b; Rennie et al., 2009a). In addition, south-westerly wind-driven upwelling events and enhanced vertical transport caused by eddy features within the Perth Canyon walls may bring nutrients close enough to the DCM for biomass maxima to form (Rennie et al., 2009b). In winter, the stronger Leeuwin Current pushes down the nitracline (Feng et al., 2009), potentially decoupling the DCM from its nutrient source and thus, increasing the formation of photo-acclimation maxima. Interestingly, the existence of thin shallow DBMs in winter fits the discovery of a thin nitrate layer off Western Australia, which forms under the Leeuwin Current independently of the deep nitracline (through nitrification) and sometimes reaches the euphotic zone within our study area (Thompson et al., 2011b).

The seasonal changes in the functional relationships between surface and depth-integrated chlorophyll reflect the seasonal patterns in water stratification and DCM formation. Low surface chlorophyll levels and deeper DCMs characterised the stratified water column in summer-transition months. These deeper DCMs are likely less intense (Cornec et al., 2021), explaining the relatively gentle regression slope (0.341). Conditions changed with the onset of a phytoplankton surface bloom in May, which is distinct for our study area (e.g., Koslow et al., 2008; Chen et al., 2020) and marks the start of the mid-winter

https://doi.org/10.5194/egusphere-2024-859
Preprint. Discussion started: 3 April 2024

season during which mixed and stratified water conditions alternate. Graff and Behrenfeld (2018) found that deep water entrainment followed by re-stratification in the North Atlantic rapidly increased surface chlorophyll (and phytoplankton biomass) over three days post-entrainment event, while chlorophyll decreased at a much slower rate at depth. Hence, changes in surface chlorophyll contributed more strongly to changing depth-integrated values. Similar processes may be at play during post-storm periods in our study area, accounting for the steeper slope derived from stratified water profiles in mid-winter (i.e., 0.433). The strong relationship with an even steeper slope (0.521) and little error in mixed water conditions reflects the homogenous vertical distribution of chlorophyll present under these conditions (Morel and Berthon, 1989; Uitz et al., 2006). Extending chlorophyll integrations to twice the euphotic zone depth showed similar functional relationships, albeit with a higher MAE, especially in summer-transition months. Scatter in the data at low surface chlorophyll values has previously been attributed to the presence of DCMs (Morel and Berthon, 1989; Uitz et al., 2006), which similarly could explain the increase in scatter for deep depth-integrated values observed here. However, we may have introduced additional errors with our definition of the euphotic zone depth as $Z_{1\%}^{PAR}$ and simple extension to "twice the euphotic zone depth". At low- and mid-latitudes specifically, $Z_{1\%}^{PAR}$ likely underestimates the compensation depth and so, $Z_{0.5\%}^{PAR}$, $Z_{0.9\%}^{USR}$ (i.e., depth at which 0.9 % of surface solar radiation is available; 400–560 nm), or $Z_{1.5\%}^{490}$ (i.e., depth at which 1.5 % of surface downwelling irradiance is available; 490 nm) have been suggested as more robust alternatives (Wu et al., 2021). Euphotic zone depth estimates based on these alternative definitions do not vary in lockstep with those based on $Z_{1\%}^{PAR}$ (Wu et al., 2021), so using a more appropriate definition of the euphotic zone may decrease the scatter observed. A lesser-known source of variation may have come from inter-annual variation in productivity, which in our study area is primarily related to fluctuations in the Leeuwin Current strength following the El Niño Southern Oscillation (ENSO; Feng et al., 2009; Chen et al., 2019). Three strong ENSO events occurred during the study period (i.e., one El Niño and two La Niña's; Australian Bureau of Meteorology, 2023), and we recommend that their effects on the relationships found are further assessed. Finally, Roessler et al. (2017) recently found that factory-calibrated chlorophyll concentrations, as estimated by optical sensors, overestimate measured chlorophyll on average by a factor of 2. While a study on the northwest Western Australian shelf, which has a similar phytoplankton community as found in the Perth Canyon, showed good agreement between chlorophyll concentrations from optical sensors and HPLC-derived chlorophyll from simultaneously collected water samples (R^2 = 0.75, slope factor = 1.2; Thomson et al., 2015), we highlight the need for a similar comparative study in the area of interest. Despite these potential sources of variation, the MAEs for relationships over twice the euphotic zone depth remained low for all three conditions (i.e., 16.3 %, 15.7 %, and 8.6 %). Arguably, the small coefficient of determination (R^2) obtained for the summer-transition regression disputes surface chlorophyll as a valuable predictor of deep depth-integrated values. However, the coefficient of determination can be misinterpreted for small data ranges, such as ours (Seegers et al., 2018).

Interestingly, we observed a third increase in mean deep depth-integrated chlorophyll in January, which was not registered at the surface or within the euphotic zone. DCMs at this time of year were predominantly DBMs and so, this deep subsurface increase may be essential for the development of krill in the study area since food availability is a crucial driver of Euphausiid health (i.e., lipid content; Fisher et al., 2020; Hellessey et al., 2020; Steinke et al., 2021), timing of reproduction (Quetin and

https://doi.org/10.5194/egusphere-2024-859
Preprint. Discussion started: 3 April 2024

Ross, 2001; Schmidt et al., 2012), hatching success (Yoshida et al., 2011; Steinke et al., 2021), and growth rate (Bahlburg et al., 2023). In fact, spawning events in several species are associated with phytoplankton blooms (e.g., Paul et al., 1990; Feinberg and Peterson, 2003; Plourde et al., 2011), after which it may take several months to years for individuals to reach sexual maturity (e.g., Boysen and Buchholz, 1984; Siegel and Loeb, 1994; Saunders et al., 2013). Baleen whales show a preference for krill >16 mm (Croll et al., 2005; Cade et al., 2022), and consequently, peak abundances of foraging baleen whales reportedly lag the onset or peak intensity of phytoplankton blooms by one to four months (Croll et al., 2005; Visser et al., 2011; Ramp et al., 2015; Abrahms et al., 2019). Sighting rates of foraging pygmy blue whales in the Perth Canyon peak in March–April (i.e., late summer to early autumn; Double et al., 2014), approximately 2–3 months after the observed increase in mean deep depth-integrated chlorophyll. These results suggest that warm summer temperatures and a deep productivity increase in January may create optimal conditions for the onset of spawning and rapid larval development in *E. recurva* with a consequent sufficient krill abundance 2–3 months later. Alternatively, as Rennie et al. (2009b) suggested, the winter surface and summer sub-surface phytoplankton bloom may additively contribute to a peak krill abundance at the end of summer and early autumn.

If the aim is to look at productivity patterns from satellite remote sensing, the question remains whether satellite-derived surface chlorophyll measurements were estimated with an acceptable error. Our validation shows that satellite-derived surface chlorophyll values estimated measured values with a mean error of 32 %, which falls within the generally accepted 35 % for satellite remote-sensing chlorophyll products (Hooker and McClain, 2000). Satellite and in situ measurements commonly differ because of the spatial (i.e., 3×3 block vs. point measurement) and temporal (here max. 24 h) mismatch of samples (Werdell et al., 2018), which likely plays an influential role in our study area where oceanic processes change the water column structure and associated surface chlorophyll at small spatial- and temporal scales (Rennie et al., 2009a; Chen et al., 2020). While strict exclusion criteria for satellite data may reduce discrepancies, we followed a standardised exclusion protocol with flexible criteria to maximise the number of matches (Concha et al., 2021). It should be noted that our sample size is small, and MAEs are not robust when based on small sample sizes (Chai and Draxler, 2014). Recalculation of the MAE as increased matches become available is therefore encouraged to ensure error measurement stability.

5 Conclusion

This study provides critical insights into the potential and need to monitor deep depth-integrated primary productivity patterns with satellite remote sensing data in regions where DCMs occur. Based on our results, we suggest including satellite-derived deep depth-integrated chlorophyll estimates in future efforts to identify productivity hotspots and anomalies off Western Australia to help better understand the relationships between productivity patterns and marine animal presence, such as foraging pygmy blue whales. Similar methods can be applied to other (intermittent) oligotrophic areas where DCMs may be an important feature for higher trophic levels. However, while our regression line slopes for the euphotic zone closely resemble those previously obtained from stratified (range 0.310–0.425 for Chl_{zpd}<1 mg m^{-3}; Morel and Berthon, 1989; Uitz et al., 2006;

https://doi.org/10.5194/egusphere-2024-859
Preprint. Discussion started: 3 April 2024

Frolov et al., 2012) and mixed water samples (0.551 and 0.538; Morel and Berthon, 1989; Uitz et al., 2006), it is clear that regression parameters need to be locally tuned and that a redefinition of the euphotic zone depth to a more biologically important definition may be required.

Data availability

All raw ocean glider data (i.e., IMOS – Australian National Facility for Ocean Gliders (ANFOG) – delayed mode glider deployments), subsetted to the spatial extent in this manuscript, are openly available from the Australian Ocean Data Network portal at https://portal.aodn.org.au/. The extracted vertical profiles used for data analysis in this study are available from the corresponding author upon request.

Author contributions

Author Contributions: RPS: Conceptualisation, methodology, coding, data acquisition & analysis, visualisation, original draft preparation, reviewing & editing; CE: Conceptualisation (supporting), supervision, reviewing & editing; RDM: Conceptualisation (supporting), supervision, reviewing & editing.

Competing interests

The authors declare that they have no conflict of interest.

Financial support

We acknowledge the Australian Government's support through an Australian Government Research Training Program Scholarship awarded to RPS.

Acknowledgements

We would like to acknowledge the Integrated Marine Observing System's Australian National Facility for Ocean Gliders (IMOS-ANFOG), from which ocean glider data used in this study was sourced. IMOS is enabled by the National Collaborative Research Infrastructure Strategy (NCRIS) and is operated by a consortium of institutions as an unincorporated joint venture, with the University of Tasmania as a lead agent. Credit should also be given to the University of Western Australia (UWA) as the operating institution of ANFOG. Thank you to David Antoine for reading through the final draft and providing meaningful feedback throughout the development of this manuscript.

https://doi.org/10.5194/egusphere-2024-859
Preprint. Discussion started: 3 April 2024

References

Abrahms, B., Hazen, E. L., Aikens, E. O., Savoca, M. S., Goldbogen, J. A., Bograd, S. J., Jacox, M. G., Irvine, L. M., Palacios, D. M., and Mate, B. R.: Memory and resource tracking drive blue whale migrations, Proc Natl Acad Sci U S A, 116, 5582–5587, https://doi.org/10.5441/001/1.5ph88fk2, 2019.

Australian Bureau of Meteorology: Climate driver update: Climate drivers in the Pacific, Indian and Southern Oceans and the tropics, last accessed October 11, 2023: http://www.bom.gov.au/climate/enso/#tabs=Indian-Ocean, 2023.

Bahlburg, D., Thorpe, S. E., Meyer, B., Berger, U., and Murphy, E. J.: An intercomparison of models predicting growth of Antarctic krill (*Euphausia superba*): The importance of recognizing model specificity, PLoS One, 18, e0286036, https://doi.org/10.1371/journal.pone.0286036, 2023.

Bailey, S. W. and Werdell, P. J.: A multi-sensor approach for the on-orbit validation of ocean color satellite data products, Remote Sens Environ, 102, 12–23, https://doi.org/10.1016/j.rse.2006.01.015, 2006.

Boettger, D., Robertson, R., and Brassington, G. B.: Verification of the mixed layer depth in the OceanMAPS operational forecast model for Austral autumn, Geosci Model Dev, 11, 3795–3805, https://doi.org/10.5194/gmd-11-3795-2018, 2018.

de Boyer Montégut, C., Madec, G., Fischer, A. S., Lazar, A., and Iudicone, D.: Mixed layer depth over the global ocean: An examination of profile data and a profile-based climatology, J Geophys Res Oceans, 109, C12003, https://doi.org/10.1029/2004JC002378, 2004.

Boysen, E. and Buchholz, F.: *Meganyctiphanes norvegica* in the Kattegat, Mar Biol, 79, 195–207, https://doi.org/10.1007/BF00951828, 1984.

Cade, D. E., Kahane-Rapport, S. R., Wallis, B., Goldbogen, J. A., and Friedlaender, A. S.: Evidence for size-selective predation by Antarctic humpback whales, Front Mar Sci, 9, 747788, https://doi.org/10.3389/fmars.2022.747788, 2022.

Chai, T. and Draxler, R. R.: Root mean square error (RMSE) or mean absolute error (MAE)? — Arguments against avoiding RMSE in the literature, Geosci Model Dev, 7, 1247–1250, https://doi.org/10.5194/gmd-7-1247-2014, 2014.

Chen, M., Pattiaratchi, C. B., Ghadouani, A., and Hanson, C.: Seasonal and inter-annual variability of water column properties along the Rottnest continental shelf, south-west Australia, Ocean Science, 15, 333–348, https://doi.org/10.5194/os-15-333-2019, 2019.

Chen, M., Pattiaratchi, C. B., Ghadouani, A., and Hanson, C.: Influence of storm events on chlorophyll distribution along the oligotrophic continental shelf off south-western Australia, Front Mar Sci, 7, 287, https://doi.org/10.3389/fmars.2020.00287, 2020.

Cohen, D. L. and Beckley, L. E.: Diet and prey selectivity of the mesopelagic lanternfish *Myctophum asperum* from the Perth Canyon, Western Australia, Ichthyol Res, 68, 294–302, https://doi.org/10.1007/s10228-020-00782-2, 2021.

Concha, J. A., Bracaglia, M., and Brando, V. E.: Assessing the influence of different validation protocols on ocean colour match-up analyses, Remote Sens Environ, 259, 112415, https://doi.org/10.1016/j.rse.2021.112415, 2021.

https://doi.org/10.5194/egusphere-2024-859
Preprint. Discussion started: 3 April 2024

Cornec, M., Claustre, H., Mignot, A., Guidi, L., Lacour, L., Poteau, A., D'Ortenzio, F., Gentili, B., and Schmechtig, C.: Deep chlorophyll maxima in the global ocean: Occurrences, drivers and characteristics, Global Biogeochem Cycles, 35, e2020GB006759, https://doi.org/10.1029/2020GB006759, 2021.

Croll, D. A., Marinovic, B., Benson, S., Chavez, F. P., Black, N., Ternullo, R., and Tershy, B. R.: From wind to whales: Trophic links in a coastal upwelling system, Mar Ecol Prog Ser, 289, 117–130, https://doi.org/10.3354/MEPS289117, 2005.

Cullen, J. J.: Subsurface chlorophyll maximum layers: Enduring enigma or mystery solved?, Ann Rev Mar Sci, 7, 207–239, https://doi.org/10.1146/annurev-marine-010213-135111, 2015.

Davies, C., Ajani, P., Armbrecht, L., Atkins, N., Baird, M., Beard, J., Bonham, P., Burford, M., Clementson, L., Coad, P., Crawford, D., Dela-Cruz, J., Doblin, M., Duggan, S., Edgar, S., Eriksen, R., Everett, J., Furnas, M., Harrison, D., Hassler, C., Henschke, J., Hoenner, X., Ingleton, T., Jameson, I., Keesing, J., Letterme, S., McLaughlin, M., Miller, M., Moffatt, D., Moss, A., Nayar, S., Patten, N., Patten, R., Pausina, S., Proctor, R., Raes, E., Robb, M., Rothlisberg, P., Saeck, E., Scanes, P., Suthers, I., Swadling, K., Thompson, P., Thomson, P., Uribe-Palomino, J., van Ruth, P., Waite, A., Wright, S., and Richardson, A.: The Australian chlorophyll *a* database (1965-2017) - abundance and biovolume, https://doi.org/10.4225/69/586f220c3f708, 2017.

Davies, C. H., Ajani, P., Armbrecht, L., Atkins, N., Baird, M. E., Beard, J., Bonham, P., Burford, M., Clementson, L., Coad, P., Crawford, C., Dela-Cruz, J., Doblin, M. A., Edgar, S., Eriksen, R., Everett, J. D., Furnas, M., Harrison, D. P., Hassler, C., Henschke, N., Hoenner, X., Ingleton, T., Jameson, I., Keesing, J., Leterme, S. C., James McLaughlin, M., Miller, M., Moffatt, D., Moss, A., Nayar, S., Patten, N. L., Patten, R., Pausina, S. A., Proctor, R., Raes, E., Robb, M., Rothlisberg, P., Saeck, E. A., Scanes, P., Suthers, I. M., Swadling, K. M., Talbot, S., Thompson, P., Thomson, P. G., Uribe-Palomino, J., Van Ruth, P., Waite, A. M., Wright, S., and Richardson, A. J.: A database of chlorophyll *a* in Australian waters, Sci Data, 5, 180018, https://doi.org/10.1038/sdata.2018.18, 2018.

Double, M. C., Andrews-Goff, V., Jenner, K. C. S., Jenner, M. N., Laverick, S. M., Branch, T. A., and Gales, N. J.: Migratory movements of pygmy blue whales (*Balaenoptera musculus brevicauda)* between Australia and Indonesia as revealed by satellite telemetry, PLoS One, 9, e95378, https://doi.org/10.1371/journal.pone.0093578, 2014.

Fang, F. and Morrow, R.: Evolution, movement and decay of warm-core Leeuwin Current eddies, Deep Sea Res 2 Top Stud Oceanogr, 50, 2245–2261, https://doi.org/10.1016/S0967-0645(03)00055-9, 2003.

Fearns, P. R., Twomey, L., Zakiyah, U., Helleren, S., Vincent, W., and Lynch, M. J.: The Hillarys transect (3): Optical and chlorophyll relationships across the continental shelf off Perth, Cont Shelf Res, 27, 1719–1746, https://doi.org/10.1016/j.csr.2007.02.004, 2007.

Feinberg, L. R. and Peterson, W. T.: Variability in duration and intensity of euphausiid spawning off central Oregon, 1996–2001, Prog Oceanogr, 57, 363–379, https://doi.org/10.1016/s0079-6611(03)00106-X, 2003.

Feng, M., Waite, A. M., and Thompson, P. A.: Climate variability and ocean production in the Leeuwin Current system off the west coast of Western Australia, J R Soc West Aust, 92, 67–81, 2009.

https://doi.org/10.5194/egusphere-2024-859
Preprint. Discussion started: 3 April 2024

Fernand, L., Weston, K., Morris, T., Greenwood, N., Brown, J., and Jickells, T.: The contribution of the deep chlorophyll maximum to primary production in a seasonally stratified shelf sea, the North Sea, Biogeochemistry, 113, 153–166, https://doi.org/10.1007/s10533-013-9831-7, 2013.

Fisher, J. L., Menkel, J., Copeman, L., Shaw, C. T., Feinberg, L. R., and Peterson, W. T.: Comparison of condition metrics and lipid content between *Euphausia pacifica* and *Thysanoessa spinifera* in the northern California Current, USA, Prog Oceanogr, 188, 102417, https://doi.org/10.1016/j.pocean.2020.102417, 2020.

Frolov, S., Ryan, J. P., and Chavez, F. P.: Predicting euphotic-depth-integrated chlorophyll-*a* from discrete-depth and satellite-observable chlorophyll-*a* off central California, J Geophys Res Oceans, 117, C05042, https://doi.org/10.1029/2011JC007322, 2012.

Gieskes, W. W. C. and Kraay, G. W.: Continuous plankton records: Changes in the plankton of the North Sea and its eutrophic southern bight from 1948 to 1975, Netherlands Journal of Sea Research, 11, 334–364, https://doi.org/10.1016/0077-7579(77)90014-X, 1977.

Gordon, H. R. and McCluney, W. R.: Estimation of the depth of sunlight penetration in the sea for remote sensing, Appl Opt, 14, 413–416, https://doi.org/10.1364/AO.14.000413, 1975.

Graff, J. R. and Behrenfeld, M. J.: Photoacclimation responses in subarctic Atlantic phytoplankton following a natural mixing-restratification event, Front Mar Sci, 5, 209, https://doi.org/10.3389/fmars.2018.00209, 2018.

Groom, S., Sathyendranath, S., Ban, Y., Bernard, S., Brewin, R., Brotas, V., Brockmann, C., Chauhan, P., Choi, J. K., Chuprin, A., Ciavatta, S., Cipollini, P., Donlon, C., Franz, B., He, X., Hirata, T., Jackson, T., Kampel, M., Krasemann, H., Lavender, S., Pardo-Martinez, S., Mélin, F., Platt, T., Santoleri, R., Skakala, J., Schaeffer, B., Smith, M., Steinmetz, F., Valente, A., and Wang, M.: Satellite ocean colour: Current status and future perspective, Front Mar Sci, 6, 485, https://doi.org/10.3389/fmars.2019.00485, 2019.

Hanson, C. E., Pattiaratchi, C. B., and Waite, A. M.: Seasonal production regimes off south-western Australia: Influence of the Capes and Leeuwin currents on phytoplankton dynamics, Mar Freshw Res, 56, 1011–1026, https://doi.org/10.1071/MF04288, 2005a.

Hanson, C. E., Pattiaratchi, C. B., and Waite, A. M.: Sporadic upwelling on a downwelling coast: Phytoplankton responses to spatially variable nutrient dynamics off the Gascoyne region of Western Australia, Cont Shelf Res, 25, 1561–1582, https://doi.org/10.1016/j.csr.2005.04.003, 2005b.

Hanson, C. E., Pesant, S., Waite, A. M., and Pattiaratchi, C. B.: Assessing the magnitude and significance of deep chlorophyll maxima of the coastal eastern Indian Ocean, Deep Sea Res 2 Top Stud Oceanogr, 54, 884–901, https://doi.org/10.1016/j.dsr2.2006.08.021, 2007.

Hellessey, N., Johnson, R., Ericson, J. A., Nichols, P. D., Kawaguchi, S., Nicol, S., Hoem, N., and Virtue, P.: Antarctic krill lipid and fatty acid content variability is associated to satellite derived chlorophyll *a* and sea surface temperatures, Sci Rep, 10, 6060, https://doi.org/10.1038/s41598-020-62800-7, 2020.

https://doi.org/10.5194/egusphere-2024-859
Preprint. Discussion started: 3 April 2024

Hobday, A. J. and Hartog, J. R.: Derived ocean features for dynamic ocean management, Oceanography, 27, 134–145, https://doi.org/10.5670/oceanog.2014.92, 2014.

Hodson, T. O.: Root-mean-square error (RMSE) or mean absolute error (MAE): When to use them or not, Geosci Model Dev, 15, 5481–5487, https://doi.org/10.5194/gmd-15-5481-2022, 2022.

Hooker, S. B. and McClain, C. R.: The calibration and validation of SeaWiFS data, Prog Oceanogr, 45, 427–465, https://doi.org/10.1016/S0079-6611(00)00012-4, 2000.

Hovis, W. A., Clark, D. K., Anderson, F., Austin, R. W., Wilson, W. H., Baker, E. T., Ball, D., Gordon, H. R., Mueller, J. L., El-Sayed, S. Z., Sturm, B., Wrigley, R. C., and Yentsch, C. S.: Nimbus-7 coastal zone color scanner: System description and initial imagery, Science (1979), 210, 60–63, https://doi.org/10.1126/science.210.4465.60, 1980.

Hu, C., Lee, Z., and Franz, B.: Chlorophyll *a* algorithms for oligotrophic oceans: A novel approach based on three-band reflectance difference, J Geophys Res Oceans, 117, C01011, https://doi.org/10.1029/2011JC007395, 2012.

Hu, C., Feng, L., Lee, Z., Franz, B. A., Bailey, S. W., Werdell, P. J., and Proctor, C. W.: Improving satellite global chlorophyll *a* data products through algorithm refinement and data recovery, J Geophys Res Oceans, 124, 1524–1543, https://doi.org/10.1029/2019JC014941, 2019.

Huot, Y., Babin, M., Bruyant, F., Grob, C., Twardowski, M. S., and Claustre, H.: Does chlorophyll *a* provide the best index of phytoplankton biomass for primary productivity studies?, Biogeosciences Discussions, 4, 707–745, https://doi.org/10.5194/bg-4-853-2007, 2007.

IMOS: IMOS - Australian Facility for Ocean Gliders (ANFOG) — delayed mode glider deployments, last accessed July 26, 2023: https://portal.aodn.org.au, 2023.

IOC, SCOR, and IAPSO: The international thermodynamic equation of seawater - 2010: Calculation and use of thermodynamic properties, Intergovernmental Oceanographic Commission, Manuals and Guides, UNESCO, Paris, France, last accessed August 4, 2023: https://www.teos-10.org/pubs/TEOS-10_Manual.pdf, 2010.

Jeffrey, S. W.: Profiles of photosynthetic pigments in the Ocean using thin-layer chromatography, Mar Biol, 26, 101–110, https://doi.org/10.1007/BF00388879, 1974.

Jeffrey, S. W., Wright, S. W., and Zapata, M.: Recent advances in HPLC pigment analysis of phytoplankton, Mar Freshw Res, 50, 879–896, https://doi.org/10.1071/MF99109, 1999.

Kara, A. B., Rochford, P. A., and Hurlburt, H. E.: Mixed layer depth variability over the global ocean, J Geophys Res Oceans, 108, 3079, https://doi.org/10.1029/2000jc000736, 2003.

Koslow, J. A., Pesant, S., Feng, M., Pearce, A., Fearns, P., Moore, T., Matear, R., and Waite, A.: The effect of the Leeuwin current on phytoplankton biomass and production off southwestern Australia, J Geophys Res Oceans, 113, C07050, https://doi.org/10.1029/2007JC004102, 2008.

Legendre, P.: Lmodel2: Model II regression. R package version 1.7.3, last accessed September 21, 2023: https://CRAN.R-project.org/package=lmodel2, 2018.

https://doi.org/10.5194/egusphere-2024-859
Preprint. Discussion started: 3 April 2024

Li, X., Mao, Z., Zheng, H., Zhang, W., Yuan, D., Li, Y., Wang, Z., and Liu, Y.: Process-oriented estimation of chlorophyll-*a* vertical profile in the Mediterranean Sea using MODIS and oceanographic float products, Front Mar Sci, 9, 933680, https://doi.org/10.3389/fmars.2022.933680, 2022.

Lourey, M. J., Dunn, J. R., and Waring, J.: A mixed-layer nutrient climatology of Leeuwin current and Western Australian shelf waters: Seasonal nutrient dynamics and biomass, Journal of Marine Systems, 59, 25–51, https://doi.org/10.1016/j.jmarsys.2005.10.001, 2006.

Marañón, E., Van Wambeke, F., Uitz, J., Boss, E. S., Dimier, C., Dinasquet, J., Engel, A., Haëntjens, N., Pérez-Lorenzo, M., Taillandier, V., and Zäncker, B.: Deep maxima of phytoplankton biomass, primary production and bacterial production in the Mediterranean Sea, Biogeosciences, 18, 1749–1767, https://doi.org/10.5194/bg-18-1749-2021, 2021.

McClain, C. R.: Satellite remote sensing: Ocean color, in: Encyclopedia of Ocean Sciences, edited by: Steele, J. H., Academic Press, San Diego, CA, United States, 114–126, 2009.

McDougall, T. J. and Barker, P. M.: Getting started with TEOS-10 and the Gibbs Seawater (GSW) Oceanographic Toolbox version 3.06.12, SCOR/IAPSO, 1–28 pp., last accessed August 4, 2023: https://www.teos-10.org/pubs/Getting_Started.pdf, 2020.

Mignot, A., Claustre, H., Uitz, J., Poteau, A., D'Ortenzio, F., and Xing, X.: Understanding the seasonal dynamics of phytoplankton biomass and the deep chlorophyll maximum in oligotrophic environments: A bio-argo float investigation, Global Biogeochem Cycles, 28, 856–876, https://doi.org/10.1002/2013GB004781, 2014.

Morel, A. and Berthon, J. F.: Surface pigments, algal biomass profiles, and potential production of the euphotic layer: Relationships reinvestigated in view of remote-sensing applications, Limnol Oceanogr, 34, 1545–1562, https://doi.org/10.4319/lo.1989.34.8.1545, 1989.

Morel, A. and Maritorena, S.: Bio-optical properties of oceanic waters: A reappraisal, J Geophys Res Oceans, 106, 7163–7180, https://doi.org/10.1029/2000jc000319, 2001.

Morel, A. and Prieur, L.: Analysis of variations in ocean color, Limnol Oceanogr, 22, 709–722, https://doi.org/10.4319/lo.1977.22.4.0709, 1977.

O'Reilly, J. E. and Werdell, P. J.: Chlorophyll algorithms for ocean color sensors - OC4, OC5 & OC6, Remote Sens Environ, 229, 32–47, https://doi.org/10.1016/j.rse.2019.04.021, 2019.

Palacios, D. M., Bailey, H., Becker, E. A., Bograd, S. J., DeAngelis, M. L., Forney, K. A., Hazen, E. L., Irvine, L. M., and Mate, B. R.: Ecological correlates of blue whale movement behavior and its predictability in the California Current Ecosystem during the summer-fall feeding season, Mov Ecol, 7, 26, https://doi.org/10.1186/s40462-019-0164-6, 2019.

Parsons, T. T. and Strickland, J. D. H.: Discussion of spectrophotometric determination of marine-plant pigments, with revised equations for ascertaining chlorophylls and carotenoids, J Mar Res, 21, 155–163, 1963.

Paul, A. J., Coyle, K. O., and Ziemann, D. A.: Timing of spawning of *Thysanoessa raschii* (Euphausiacea) and occurrence of their feeding-stage larvae in an Alaskan Bay, Journal of Crustacean Biology, 10, 69–78, https://doi.org/10.1163/193724090X00258, 1990.

https://doi.org/10.5194/egusphere-2024-859
Preprint. Discussion started: 3 April 2024

Pearce, A. F. and Griffiths, R. W.: The mesoscale structure of the Leeuwin Current: a comparison of laboratory models and satellite imagery, J Geophys Res Oceans, 96, 16739–16757, https://doi.org/10.1029/91jc01712, 1991.

Plourde, S., Winkler, G., Joly, P., St-Pierre, J. F., and Starr, M.: Long-term seasonal and interannual variations of krill spawning in the lower St Lawrence estuary, Canada, 1979-2009, J Plankton Res, 33, 703–714, https://doi.org/10.1093/plankt/fbq144, 2011.

Quetin, L. B. and Ross, R. M.: Environmental variability and its impact on the reproductive cycle of Antarctic krill, Am Zool, 41, 74–89, https://doi.org/10.1093/icb/41.1.74, 2001.

R Core Team: R: A language and environment for statistical computing, last accessed September 19, 2023: https://www.R-project.org/, 2022.

Ramp, C., Delarue, J., Palsbøll, P. J., Sears, R., and Hammond, P. S.: Adapting to a warmer ocean—Seasonal shift of baleen whale movements over three decades, PLoS One, 10, e0121374, https://doi.org/10.1371/journal.pone.0121374, 2015.

Rennie, S., Hanson, C. E., McCauley, R. D., Pattiaratchi, C., Burton, C., Bannister, J., Jenner, C., and Jenner, M. N.: Physical properties and processes in the Perth Canyon, Western Australia: Links to water column production and seasonal pygmy blue whale abundance, Journal of Marine Systems, 77, 21–44, https://doi.org/10.1016/j.jmarsys.2008.11.008, 2009a.

Rennie, S. J., McCauley, R. D., and Pattiaratchi, C. B.: Thermal structure above the Perth Canyon reveals Leeuwin Current, undercurrent and weather influences and the potential for upwelling, Mar Freshw Res, 57, 849–861, https://doi.org/10.1071/MF05247, 2006.

Rennie, S. J., Pattiaratchi, C. B., and McCauley, R. D.: Numerical simulation of the circulation within the Perth Submarine Canyon, Western Australia, Cont Shelf Res, 29, 2020–2036, https://doi.org/10.1016/j.csr.2009.04.010, 2009b.

Roesler, C., Uitz, J., Claustre, H., Boss, E., Xing, X., Organelli, E., Briggs, N., Bricaud, A., Schmechtig, C., Poteau, A., D'Ortenzio, F., Ras, J., Drapeau, S., Haëntjens, N., and Barbieux, M.: Recommendations for obtaining unbiased chlorophyll estimates from *in situ* chlorophyll fluorometers: A global analysis of WET Labs ECO sensors, Limnol Oceanogr Methods, 15, 572–585, https://doi.org/10.1002/lom3.10185, 2017.

Roesler, C. S. and Barnard, A. H.: Optical proxy for phytoplankton biomass in the absence of photophysiology: Rethinking the absorption line height, Methods in Oceanography, 7, 79–94, https://doi.org/10.1016/j.mio.2013.12.003, 2013.

Salgado Kent, C., Bouchet, P., Wellard, R., Parnum, I., Fouda, L., and Erbe, C.: Seasonal productivity drives aggregations of killer whales and other cetaceans over submarine canyons of the Bremer Sub-Basin, south-western Australia, Aust Mammal, 43, 168–178, https://doi.org/10.1071/AM19058, 2020.

Sathyendranath, S., Brewin, R. J. W., Brockmann, C., Brotas, V., Calton, B., Chuprin, A., Cipollini, P., Couto, A. B., Dingle, J., Doerffer, R., Donlon, C., Dowell, M., Farman, A., Grant, M., Groom, S., Horseman, A., Jackson, T.,

https://doi.org/10.5194/egusphere-2024-859
Preprint. Discussion started: 3 April 2024

Krasemann, H., Lavender, S., Martinez-Vicente, V., Mazeran, C., Mélin, F., Moore, T. S., Müller, D., Regner, P., Roy, S., Steele, C. J., Steinmetz, F., Swinton, J., Taberner, M., Thompson, A., Valente, A., Zühlke, M., Brando, V. E., Feng, H., Feldman, G., Franz, B. A., Frouin, R., Gould Jr, R. W., Hooker, S. B., Kahru, M., Kratzer, S., Mitchell, B. G., Muller-Karger, F. E., Sosik, H. M., Voss, K. J., Werdell, J., and Platt, T.: An ocean-colour time series for use in climate studies: The experience of the ocean-colour climate change initiative (OC-CCI), Sensors, 19, 4285, https://doi.org/10.3390/s19194285, 2019.

Saunders, R. A., Rasmussen, J., Tarling, G. A., and Brierley, A. S.: Distribution, population dynamics and growth rates of *Thysanopoda acutifrons*, *Thysanoessa inermis* and *Nematobrachion boöpis* in the Irminger Sea, North Atlantic, Journal of the Marine Biological Association of the United Kingdom, 93, 1287–1301, https://doi.org/10.1017/S0025315412001385, 2013.

Schmidt, K., Atkinson, A., Venables, H. J., and Pond, D. W.: Early spawning of Antarctic krill in the Scotia Sea is fuelled by "superfluous" feeding on non-ice associated phytoplankton blooms, Deep Sea Res 2 Top Stud Oceanogr, 59–60, 159–172, https://doi.org/10.1016/j.dsr2.2011.05.002, 2012.

Scott, B. E., Sharples, J., Ross, O. N., Wang, J., Pierce, G. J., and Camphuysen, C. J.: Sub-surface hotspots in shallow seas: Fine-scale limited locations of top predator foraging habitat indicated by tidal mixing and sub-surface chlorophyll, Mar Ecol Prog Ser, 408, 207–226, https://doi.org/10.3354/meps08552, 2010.

Seegers, B. N., Stumpf, R. P., Schaeffer, B. A., Loftin, K. A., and Werdell, P. J.: Performance metrics for the assessment of satellite data products: An ocean color case study, Opt Express, 26, 7404, https://doi.org/10.1364/OE.26.007404, 2018.

Siegel, V. and Loeb, V.: Length and age at maturity of Antarctic krill, Antarct Sci, 6, 479–482, https://doi.org/10.1017/s0954102094000726, 1994.

Smith, R. C.: Remote sensing and depth distribution of ocean chlorophyll, Mar Ecol Prog Ser, 5, 359–361, 1981.

Speakman, C. N., Hoskins, A. J., Hindell, M. A., Costa, D. P., Hartog, J. R., Hobday, A. J., and Arnould, J. P. Y.: Environmental influences on foraging effort, success and efficiency in female Australian fur seals, Sci Rep, 10, 17710, https://doi.org/10.1038/s41598-020-73579-y, 2020.

Steele, J. H.: Environmental control of photosynthesis in the sea, Limnol Oceanogr, 7, 137–150, https://doi.org/10.4319/lo.1962.7.2.0137, 1962.

Steele, J. H.: A study of production in the Gulf of Mexico, J Mar Res, 22, 211–222, 1964.

Steinke, K. B., Bernard, K. S., Ross, R. M., and Quetin, L. B.: Environmental drivers of the physiological condition of mature female Antarctic krill during the spawning season: implications for krill recruitment, Mar Ecol Prog Ser, 669, 65–82, https://doi.org/10.3354/meps13720, 2021.

Suryan, R. M., Santora, J. A., and Sydeman, W. J.: New approach for using remotely sensed chlorophyll *a* to identify seabird hotspots, Mar Ecol Prog Ser, 451, 213–225, https://doi.org/10.3354/meps09597, 2012.

https://doi.org/10.5194/egusphere-2024-859
Preprint. Discussion started: 3 April 2024

Sutton, A. L.: Krill in the Leeuwin Current system: Influence of oceanography and contribution to Indian Ocean zoogeography, PhD, Murdoch University, Perth, Western Australia, last accessed September 13, 2023: https://researchportal.murdoch.edu.au/esploro/outputs/doctoral/Krill-in-the-Leeuwin-Current-system/991005544756707891, 2015.

Sutton, A. L. and Beckley, L. E.: Influence of the Leeuwin Current on the epipelagic euphausiid assemblages of the south-east Indian Ocean, Hydrobiologia, 779, 193–207, https://doi.org/10.1007/s10750-016-2814-7, 2016.

The MathWorks Inc.: MATLAB version: 9.13.0 (R2022b), last accessed October 12, 2023: https://www.mathworks.com/?s_tid=gn_logo, 2022.

Thieurmel, B. and Elmarhraoui, A.: Suncalc: Compute sun position, sunlight phases, moon position, and lunar phase. R package version 0.5.1, last accessed September 19, 2023: https://CRAN.R-project.org/package=suncalc, 2022.

Thompson, P. A., Pesant, S., and Waite, A. M.: Contrasting the vertical differences in the phytoplankton biology of a dipole pair of eddies in the south-eastern Indian Ocean, Deep Sea Res 2 Top Stud Oceanogr, 54, 1003–1028, https://doi.org/10.1016/j.dsr2.2006.12.009, 2007.

Thompson, P. A., Bonham, P., Waite, A. M., Clementson, L. A., Cherukuru, N., Hassler, C., and Doblin, M. A.: Contrasting oceanographic conditions and phytoplankton communities on the east and west coasts of Australia, Deep Sea Res 2 Top Stud Oceanogr, 58, 645–663, https://doi.org/10.1016/j.dsr2.2010.10.003, 2011a.

Thompson, P. A., Wild-Allen, K., Lourey, M., Rousseaux, C., Waite, A. M., Feng, M., and Beckley, L. E.: Nutrients in an oligotrophic boundary current: Evidence of a new role for the Leeuwin Current, Prog Oceanogr, 91, 345–359, https://doi.org/10.1016/j.pocean.2011.02.011, 2011b.

Thomson, P. G., Mantovanelli, A., Wright, S. W., and Pattiaratchi, C. B.: *In situ* comparisons of glider bio-optical measurements to CTD water properties, in: Australian Marine Sciences Conference: Estuaries to Oceans, 306, 2015.

Twomey, L. J., Waite, A. M., Pez, V., and Pattiaratchi, C. B.: Variability in nitrogen uptake and fixation in the oligotrophic waters off the south west coast of Australia, Deep Sea Res 2 Top Stud Oceanogr, 54, 925–942, https://doi.org/10.1016/j.dsr2.2006.10.001, 2007.

Uitz, J., Claustre, H., Morel, A., and Hooker, S. B.: Vertical distribution of phytoplankton communities in open ocean: An assessment based on surface chlorophyll, J Geophys Res Oceans, 111, C08005, https://doi.org/10.1029/2005JC003207, 2006.

Visser, F., Hartman, K. L., Pierce, G. J., Valavanis, V. D., and Huisman, J.: Timing of migratory baleen whales at the Azores in relation to the North Atlantic spring bloom, Mar Ecol Prog Ser, 440, 267–279, https://doi.org/10.3354/meps09349, 2011.

Werdell, P. J., McKinna, L. I. W., Boss, E., Ackleson, S. G., Craig, S. E., Gregg, W. W., Lee, Z., Maritorena, S., Roesler, C. S., Rousseaux, C. S., Stramski, D., Sullivan, J. M., Twardowski, M. S., Tzortziou, M., and Zhang, X.: An overview of approaches and challenges for retrieving marine inherent optical properties from ocean color remote sensing, Prog Oceanogr, 160, 186–212, https://doi.org/10.1016/j.pocean.2018.01.001, 2018.

https://doi.org/10.5194/egusphere-2024-859
Preprint. Discussion started: 3 April 2024

Weston, K., Fernand, L., Mills, D. K., Delahunty, R., and Brown, J.: Primary production in the deep chlorophyll maximum of the central North Sea, J Plankton Res, 27, 909–922, https://doi.org/10.1093/plankt/fbi064, 2005.

Whiteway, T.: Australian bathymetry and topography grid, June 2009. Scale 1:5000000, https://doi.org/10.4225/25/53D99B6581B9A, 2009.

Woo, L. M. and Gourcuff, C.: Delayed mode QA/QC best practice manual version 3.0, Integrated Marine Observing System (IMOS), 1–60 pp., https://doi.org/10.26198/5c997b5fdc9bd, 2011.

Wu, J., Lee, Z., Xie, Y., Goes, J., Shang, S., Marra, J. F., Lin, G., Yang, L., and Huang, B.: Reconciling between optical and biological determinants of the euphotic zone depth, J Geophys Res Oceans, 126, e2020JC016874, https://doi.org/10.1029/2020JC016874, 2021.

Yentsch, C. S. and Menzel, D. W.: A method for the determination of phytoplankton chlorophyll and phaeophytin by fluorescence, Deep Sea Research and Oceanographic Abstracts, 10, 221–231, https://doi.org/10.1016/0011-7471(63)90358-9, 1963.

Yoshida, T., Virtue, P., Kawaguchi, S., and Nichols, P. D.: Factors determining the hatching success of Antarctic krill *Euphausia superba* embryo: Lipid and fatty acid composition, Mar Biol, 158, 2313–2325, https://doi.org/10.1007/s00227-011-1735-2, 2011.

Zibordi, G., Berthon, J. F., Mélin, F., D'Alimonte, D., and Kaitala, S.: Validation of satellite ocean color primary products at optically complex coastal sites: Northern Adriatic Sea, Northern Baltic Proper and Gulf of Finland, Remote Sens Environ, 113, 2574–2591, https://doi.org/10.1016/j.rse.2009.07.013, 2009.